

# Rapid Shift from Virally Infected Cells to Germinal Center-Retained Virus after HIV-2 Infection of Macaques

Frank Eitner,\* Yan Cui,\*  
Géraldine Grouard-Vogel,<sup>†</sup> Kelly L. Hudkins,\*  
Ann Schmidt,<sup>‡</sup> Ted Birkebak,<sup>‡</sup> Michael B. Agy,<sup>‡</sup>  
Shiu-Lok Hu,<sup>‡</sup> William R. Morton,<sup>‡</sup>  
David M. Anderson,<sup>‡</sup> Edward A. Clark,<sup>†</sup> and  
Charles E. Alpers\*

From the Departments of Pathology\* and Microbiology<sup>†</sup> and The Washington Regional Primate Center,<sup>‡</sup> University of Washington, Seattle, Washington

**Lymphoid tissues are the primary target during the initial virus dissemination that occurs in HIV-1-infected individuals. Recent advances in antiretroviral therapy and techniques to monitor virus load in humans have demonstrated that the early stages of viral infection and host response are major determinants of the outcome of individual infections. Relatively little is known about immunopathogenic events occurring during the acute phase of HIV infection. We analyzed viral dissemination within lymphoid tissues by *in situ* hybridization and by combined immunohistochemistry/*in situ* hybridization during the acute infection phase (12 hours to 28 days) in pig-tailed macaques (*Macaca nemestrina*), challenged intravenously with a virulent strain of HIV-2, HIV-2<sub>287</sub>. Two stages in viral dissemination were clearly evident within the first 28 days after HIV-2<sub>287</sub> infection. First, a massive increase in individual HIV-2-infected cells, mostly CD3+ T lymphocytes and a smaller percentage of macrophages and interdigitating dendritic cells, was identified within lymph nodes which peaked on the 10th day after HIV-2 infection. A shift of HIV-2 distribution was demonstrable between day 10 and day 14 after HIV-2 infection. Coincident with a marked reduction in individual HIV-2 RNA+ cells by day 14 postinfection, there was a dramatic increase in germinal center-associated HIV-2 RNA. High concentrations of HIV-2 RNA persisted in germinal centers in all animals by days 21 and 28 postinfection. Thus, HIV-2 appears to go through an initial, highly disseminated cellular phase followed by localization in the follicular dendritic cell network with relatively few infected cells. In this nonhuman primate model of HIV-associated immunopathogenesis, using a virus derived from a human pathogen, we identified a significant shift in the pattern of HIV-2 localization**

**within a narrow time frame (day 10 to day 14). This shift in virus localization and behavior indicates that there may be a discrete but remarkably narrow window for therapeutic interventions that interrupt this stage in the natural course of HIV infection. Reproducibility and the accelerated time course of disease development make this model an excellent candidate for such intervention studies. (Am J Pathol 2000, 156:1197-1207)**

Lymphoid organs are the primary anatomical sites for the initial establishment of HIV-1 infection in humans.<sup>1</sup> HIV replicates in lymphoid organs throughout the course of infection, including the generally asymptomatic, clinically latent period.<sup>2-8</sup> CD4+ T lymphocytes, monocytes/macrophages, and bone marrow derived dendritic cells are the cellular targets of HIV-1 infection.<sup>1,9</sup> In lymphoid tissues of HIV-1-infected individuals, HIV-1 RNA and protein are localized to both individual cells and to the follicular dendritic cell (FDC) network of germinal centers. Productive and latent infection occurs in T cells and macrophages, whereas FDCs retain on their surfaces large numbers of HIV-1 particles, proteins, and viral RNA, primarily as immune complexes.<sup>2-8,10</sup> Apparently, HIV does not replicate in FDCs.<sup>11-14</sup> Although much is known about the terminal phase of AIDS, relatively little is known about the acute phase of HIV infection, which may play a major role in determining disease outcome.<sup>15</sup> Investigation of the early events has been limited by difficulties in identifying and studying individuals during these early stages of infection in humans.

The identification of relevant animal models has been of central importance for evaluating phases of immunodeficiency virus pathogenesis *in vivo*.<sup>16-18</sup> We have recently characterized HIV-2<sub>287</sub>,<sup>19,20</sup> a highly pathogenic strain of HIV-2 that was recovered from a pig-tailed macaque (*Macaca nemestrina*) after serial *in vivo* passage of a parent strain, HIV-2<sub>EHO</sub>, isolated from a human AIDS patient.<sup>21</sup> HIV-2<sub>287</sub> not only is readily infectious for *M.*

---

Supported in part by grants DK 49514, DK 47659, HL 63652, and RR 00166 from the National Institutes of Health.

Accepted for publication December 13, 1999.

Address reprint requests to Charles E. Alpers, M.D., Department of Pathology, University of Washington, Box 356100, 1959 NE Pacific Street, Seattle, WA 98195. E-mail: calp@u.washington.edu.

*nemestrina*, but also is highly pathogenic, progressing to a clinical AIDS syndrome within an accelerated time frame of 6 to 12 months.<sup>19,20,22</sup> Pig-tailed macaques inoculated with HIV-2<sub>287</sub> exhibit high virus loads and rapid CD4 cell depletion within weeks after inoculation.<sup>20,22</sup> Although HIV-2 is closely related to simian immunodeficiency virus (SIV), HIV-2<sub>287</sub> remains distinct from all known strains of SIV, thereby presenting a unique opportunity for study of a macaque model of human AIDS using a virus derived from a human pathogen.

The present study is part of an in-depth evaluation of the acute events following HIV-2<sub>287</sub> infection of *M. nemestrina*. Here we prospectively analyze patterns of virus dissemination in mesenteric lymph nodes of 27 macaques between 12 hours and 28 days after intravenous HIV-2<sub>287</sub> infection. By *in situ* hybridization, maximal numbers of HIV-2 RNA+ cells were detected on day 10 after infection. Immunohistochemical labeling clearly identified the great majority (>90%) of HIV-2 RNA+ cells as T cells and smaller numbers of HIV-2 RNA+ cells as macrophages and interdigitating dendritic cells. A dramatic shift in HIV-2 distribution occurred between days 10 and 14. While there were relatively few HIV-2 RNA+ cells in mesenteric lymph nodes by day 14, a massive increase in germinal center-associated viral RNA was detected at that time point and persisted in all animals examined at 21 or 28 days postinfection.

Thus, in lymphoid tissues, HIV-2 appears to infect individual cells initially, predominantly T cells, and later localizes to the FDC network of germinal centers with relatively few individual infected cells. The rapidity of this process is striking and is a major finding of this study. An important implication of this finding is that in this model, and probably in at least some human infections with HIV, the window of opportunity for therapeutic interruption of the movement of infectious virus into reservoirs such as the FDC network, where viral latency can be achieved, occurs very early in the natural history of infection and is chronologically very short

## Materials and Methods

### Animals

Twenty-seven pig-tailed macaques (*M. nemestrina*; ages 1.2–3.1 years, median, 2.1 years; 11 male, 16 female) were inoculated intravenously with 50 TCID<sub>50</sub> (50% tissue culture infectious doses) of HIV-2<sub>287</sub>. Before inoculation, each animal was determined to be clinically healthy by physical examination and complete blood cell count and to be negative for SIV and simian retrovirus. The macaques were euthanized at 12 hours or day 1, 2, 4, 6, 10, 14, 21, or 28 ( $n = 3$  at each time point) after inoculation, and complete necropsy examinations were performed. All study protocols and procedures were reviewed and approved by the Washington Regional Primate Research Center and the University of Washington Animal Care and Use Committee. Four uninfected, untreated, clinically healthy pig-tailed macaques, *M. nemestrina* (ages 1.4–2.6 years; 3 male, 1 female), were euthanized and served

as control animals. Mesenteric lymph nodes were obtained from each macaque at necropsy. Tissue samples were fixed in 10% phosphate-buffered formalin, embedded in paraffin, and sectioned for further *in situ* hybridization studies. Additionally, mesenteric lymph node cells or total DNA were isolated for coculture or polymerase chain reaction (PCR) studies, respectively, as detailed below.

### Virus

The HIV-2 virus used in this study, HIV-2<sub>287</sub>, is described in detail elsewhere.<sup>20</sup> HIV-2<sub>287</sub> was derived by serial passage of HIV-2<sub>EHO</sub> in *M. nemestrina*.<sup>21</sup> The HIV-2<sub>287</sub> challenge stock was derived from coculture of lymph node mononuclear cells of a macaque used for the serial passage study with fresh stimulated allogenic macaque peripheral blood mononuclear cells (PBMC). Virus stocks were prepared as clarified supernatants (3000 × *g* for 20 minutes at 4°C), aliquoted and stored at –80°C until use. All 27 macaques were inoculated intravenously with 50 TCID<sub>50</sub> of this virus stock solution. This dose of HIV-2<sub>287</sub> was chosen because it has induced infection and the development of an immunodeficiency syndrome in 100% of inoculated animals in prior HIV-2<sub>287</sub> *in vivo* titration studies.<sup>22</sup>

### Hematological Parameters

Samples of EDTA-plasma were obtained from each macaque before HIV-2 inoculation and at different time points after inoculation, including immediately before experimental euthanasia. Complete blood count was measured using standard procedures. The CD4+ T cell subset was measured by staining leukocytes with PE-conjugated CD4 antibody (Leu 3a, Becton Dickinson, San Jose, CA) and analyzed using a flow cytometer (FACScan/FACSort, Becton Dickinson).

### Detection of HIV-2-Infected Mesenteric Lymph Node Cells by Coculture

HIV-2-infected PBMC were detected by a quantitative coculture assay as described.<sup>22,23</sup> Cells were harvested from several mesenteric lymph nodes simultaneously. Freshly isolated mesenteric lymph node cells were serially diluted in triplets, starting with 10<sup>6</sup> cells and cocultivated with fresh human CD8+, T-cell-depleted, PHA-activated PBMCs. Cultures were incubated for 14 days and the presence of virus was detected using an HIV-2 p27 antigen capture assay. Titers were calculated as the maximal dilution of cells which gave positive cultures and reported as numbers of HIV-2+ cells/10<sup>6</sup> mesenteric lymph node cells.

### Detection of Proviral HIV-2 DNA

Proviral HIV-2 DNA was detected by a modification of a previously described protocol.<sup>22</sup> Briefly, total DNA was

isolated from mesenteric lymph nodes and reacted with *gag*-specific primers. The primers were designated 3Q (5'-CCCAGGCATTTAAGGTTTCGGG-3') and 5Qii (5'-GGATTGGCAGAGAGCCTGTTG-3'), which generated a 334-bp product from proviral DNA. The internal competitor, tCon6, was generated by PCR as previously described.<sup>24</sup> The competitor is distinguished from the wild-type *gag* signal by a 76-bp deletion (258 vs. 334 bp). The DNA samples were serially diluted fourfold ( $n = 6$ ) and run in duplicate. Each reaction included 100 copies of tCon6 competitor. The PCR conditions began with 10 minutes' denaturation-TaqGold-activation 95°C incubation followed by three initial cycles of 15 seconds at 96°C, 30 seconds at 52°C, 30 seconds at 56°C, and 30 seconds at 72°C. These were followed by 42 cycles of 15 seconds at 95°C, 30 seconds at 58°C, and 30 seconds at 72°C, with a final 9 minutes at 72°C. The PCR products were resolved on a 2.5% agarose gel and stained with ethidium bromide, and the equivalence points were determined visually. The results were reported as copies/ $\mu$ g total DNA. Although we were able to detect levels in the 100-copy range, accurate quantitation could be determined only on samples containing  $\geq 1000$  copies.

### Antibodies

An affinity-isolated rabbit polyclonal antiserum directed against human CD3 was purchased from DAKO (Carpinteria, CA) and used on formalin-fixed, paraffin-embedded tissue sections after heat-mediated antigen retrieval.<sup>25</sup> A murine mAb Ham56 (DAKO) directed against a human macrophage marker was used to detect macaque macrophages as described previously for nonhuman primate fixed tissues.<sup>26</sup> A rabbit polyclonal antiserum to S100 (DAKO) was used to detect the cytoplasmic S100, present in FDCs and dendritic cells, in formalin-fixed, paraffin-embedded macaque tissues.<sup>27</sup> S100 is broadly expressed but is not found in lymphoid cells.<sup>28</sup> A murine mAb to Fascin/p55 recognizes a 55-kd protein found on microspikes and stress fibers in interdigitating dendritic cells within T-cell-dependent areas of lymphoid organs<sup>29</sup> (This antibody was obtained through the AIDS Research and Reference Reagent Program, Division of AIDS, National Institute of Allergy and Infectious Diseases, National Institutes of Health<sup>30</sup>). This antibody detects nonhuman primate interdigitating dendritic cells in formalin-fixed, paraffin-embedded tissue sections.<sup>31</sup>

### Molecular Probes

A 1.7-kb sequence of DNA coding for HIV-2 gp120 (*env*; nucleotides 6480–8335 of the HIV-2<sub>287</sub> sequence) was subcloned into pCR II (Invitrogen; kindly provided by Bristol-Myers Squibb, Seattle, WA), and either linearized with *Xho*I and transcribed with Sp6 RNA polymerase for the antisense probe, or linearized with *Bam*HI and transcribed with T7 RNA polymerase for the sense probe. Detailed protocols for the transcription reaction and the

characterization of the specificity of this riboprobe have been described previously.<sup>32</sup>

### In Situ Hybridization

HIV-2 RNA was detected in tissue sections using *in situ* hybridization techniques as previously described.<sup>33,34</sup> Riboprobes for *in situ* hybridization were generated from cDNA using <sup>35</sup>S-UTP (New England Nuclear, Boston, MA). Four micron sections of formalin-fixed, paraffin-embedded mesenteric lymph nodes were deparaffinized and rehydrated through xylene and graded ethanols, washed with 0.5 $\times$  SSC (Gibco, Grand Island, NY) and digested with proteinase K (5  $\mu$ g/ml; Sigma, St. Louis, MO). Prehybridization was performed for 2 hours by adding 100  $\mu$ l of prehybridization buffer (0.3 mol/L NaCl, 20 mmol/L Tris, pH 8.0, 5 mmol/L EDTA, 1 $\times$  Denhardt's solution, 10% dextran sulfate, 10 mmol/L dithiothreitol). The hybridizations were started by adding 500,000 cpm of <sup>35</sup>S-labeled riboprobe in 50  $\mu$ l of prehybridization buffer and allowed to proceed overnight at 50°C. After hybridization, sections were treated with RNase A (20  $\mu$ g/ml, Sigma), followed by three high-stringency washes in 0.1 $\times$  SSC/0.5% Tween 20 (Sigma) for 40 minutes each at 50°C, and several 2 $\times$  SSC washes. After the tissue was dehydrated and air-dried, it was dipped in NTB2 nuclear emulsion (Kodak, Rochester, NY) and exposed in the dark at 4°C. After developing, the sections were counterstained with hematoxylin and eosin, dehydrated, and coverslipped.

Total lymph node areas were determined by computer-assisted morphometry as described.<sup>35</sup> The image analysis system consisted of a microscope (Olympus BH-2, Olympus America, Melville, NY) with a high-resolution video camera (Hitachi VK-350, Hitachi, Tokyo, Japan) connected to a Pentium 100 computer equipped with a True Vision image acquisition board and video monitor (Triniton, Sony, New York, NY). Area measurements were done using the Optimas Image Analysis Software Package (Bioscan, Edmonds, WA).

### Optimization of HIV-2 RNA Detection

*In situ* hybridization procedures require pretreatment (proteinase K digestion or heat treatment in citrate buffer) of the formalin-fixed, paraffin-embedded tissue sections to increase the hybridization efficiency. Tenner-Racz et al have reported a different specificity of their HIV-1 RNA *in situ* hybridization depending on the method of pretreatment of the formalin-fixed, paraffin-embedded lymph node tissue sections.<sup>36</sup> They concluded that individual HIV-1 RNA expressing cells were visualized best after high temperature treatment. However, detection of HIV-1 RNA presumably bound to the FDC network of germinal centers depended on proteinase K digestion.<sup>36</sup>

Pilot experiments determined optimal tissue treatment conditions for the detection of HIV-2 RNA in formalin-fixed, paraffin-embedded macaque lymph node sections. In agreement with Tenner-Racz et al,<sup>36</sup> the specificity of our HIV-2 RNA detection depended on the

conditions used for tissue pretreatment. Treatment of sections with proteinase K alone (5  $\mu\text{g/ml}$ , 30 minutes, room temperature) resulted in optimal detection of individual HIV-2 RNA expressing cells. FDC-bound HIV-2 RNA was almost completely undetectable using this procedure. The combination of high temperature treatment, ie, 20 minutes steam-heating in Antigen Unmasking Solution (Vector, Burlingame, CA), and proteinase K digestion (5  $\mu\text{g/ml}$ , 30 minutes, room temperature) resulted in optimal visualization of FDC-bound HIV-2 RNA. Exposure times of 2 weeks for proteinase K treated and of 4 weeks for heat plus proteinase K treated tissue sections resulted in optimal sensitivity and specificity for the detection of individual HIV-2 RNA-expressing cells or FDC-bound HIV-2 RNA, respectively. Comparison of both methods of tissue pretreatment did not show significant differences in either signal intensity (grain counts of individual HIV-2 RNA-expressing cells), nonspecific background signal, or preservation of tissue morphology. However, the intense, diffuse labeling of FDC-bound HIV-2 RNA observed after proteinase K plus heat treatment in some analyzed specimens made the specific detection of individual HIV-2-infected cells within germinal centers impossible.

We therefore performed *in situ* hybridization for the detection of HIV-2 RNA in all cases in duplicate. The number of individual HIV-2 infected cells was analyzed in proteinase K-treated sections and FDC-bound HIV-2 RNA was analyzed in heat plus proteinase K-treated sections.

### Combined Immunohistochemistry and *in Situ* Hybridization

To further identify the phenotypes of HIV-2-infected cells, sections of mesenteric lymph nodes were immunostained for CD3 (T lymphocytes), Ham56 (macrophages), S100 (FDCs and dendritic cells), or fascin/p55 (interdigitating dendritic cells) before *in situ* hybridization. Combined immunohistochemistry and *in situ* hybridization was performed as described.<sup>37</sup> Formalin-fixed, paraffin-embedded tissues were prepared as described above. Sections that were subsequently incubated with the CD3, fascin/p55, or S100 antibodies were pretreated by steam-heating for 20 minutes in Antigen Unmasking Solution (Vector) according to the instructions of the manufacturer. The sections were then incubated for 1 hour with the primary antibody diluted in PBS containing 1% bovine serum albumin (Sigma). After washes in PBS, the sections were sequentially incubated with biotinylated goat anti-rabbit (Vector) or biotinylated horse anti-mouse antibody (Vector), the ABC-Elite reagent (Vector), and finally 3,3'-diaminobenzidine was used as the chromogen. After an overnight incubation in PBS, *in situ* hybridization for HIV-2 RNA was performed as described above. After hybridizations the sections were incubated in the dark at 4°C for 2 weeks. Negative controls for the immunohistochemical procedures consisted of substitution of the primary antibody with irrelevant, isotype-matched murine mAb (DAKO) or nonimmune rabbit serum (DAKO).

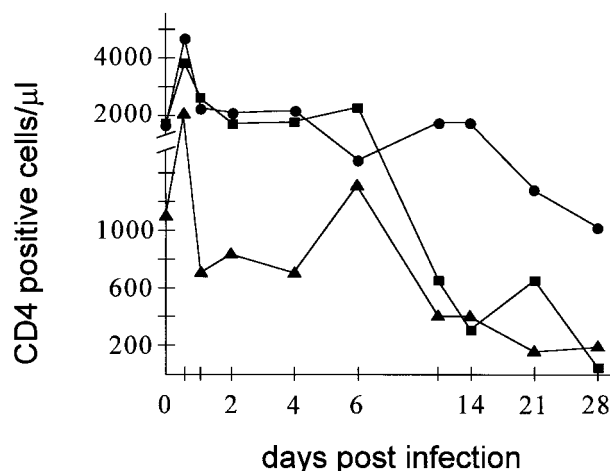


**Figure 1.** HIV-2<sub>287</sub> inoculation was associated with a rapid decline in CD4+ PBMC. Serial blood samples were obtained and analyzed for CD4+ cells as detailed in the Methods section. Graphic illustrates serial peripheral blood CD4+ cell counts before (day 0) and after HIV-2 inoculation in the three macaques that were euthanized 28 days after HIV-2 inoculation.

### Serology

Circulating levels of IgG and IgA antibodies to HIV-2 were evaluated by enhanced chemiluminescence immuno-blots using a modification of techniques previously published for detection of antibodies to SIV.<sup>38</sup>

### Results

#### HIV-2 Infection Induces an Immunodeficiency Syndrome in Pig-Tailed Macaques

Infection of pig-tailed macaques with HIV-2<sub>287</sub> resulted in a rapid and predictable decline in blood CD4+ cells. Serial blood samples obtained within the 28 days after HIV-2<sub>287</sub> inoculation demonstrated a significant decrease of CD4+ T lymphocytes (Figure 1). HIV-2 infected PBMC were detectable in PBMC cocultures in every macaque, studied 10 days or later after infection.<sup>39</sup> None of the 27 macaques involved in the study developed other features of clinical AIDS within the time frame of the study period.

#### Detection of HIV-2 RNA in Mesenteric Lymph Nodes

By *in situ* hybridization, HIV-2 RNA remained completely undetectable in lymph nodes of uninfected control animals and all macaques at 12 hours, 1 and 2 days after HIV-2 infection (Figure 2A). At day 4 and day 6 postinfection, small numbers of single HIV-2 RNA expressing cells were identified in 1 of 3 animals (Figure 2A). These cells were almost exclusively localized within the extrafollicular lymphoid tissue, including sinuses and interfollicular T-cell-dependent zones (Figure 3, A and B). Only rarely was an individual HIV-2 RNA-expressing cell detected within a germinal center at days 4 and 6 after HIV-2 infection. At day 10 postinfection, mesenteric lymph nodes of all three animals exhibited maximal num-

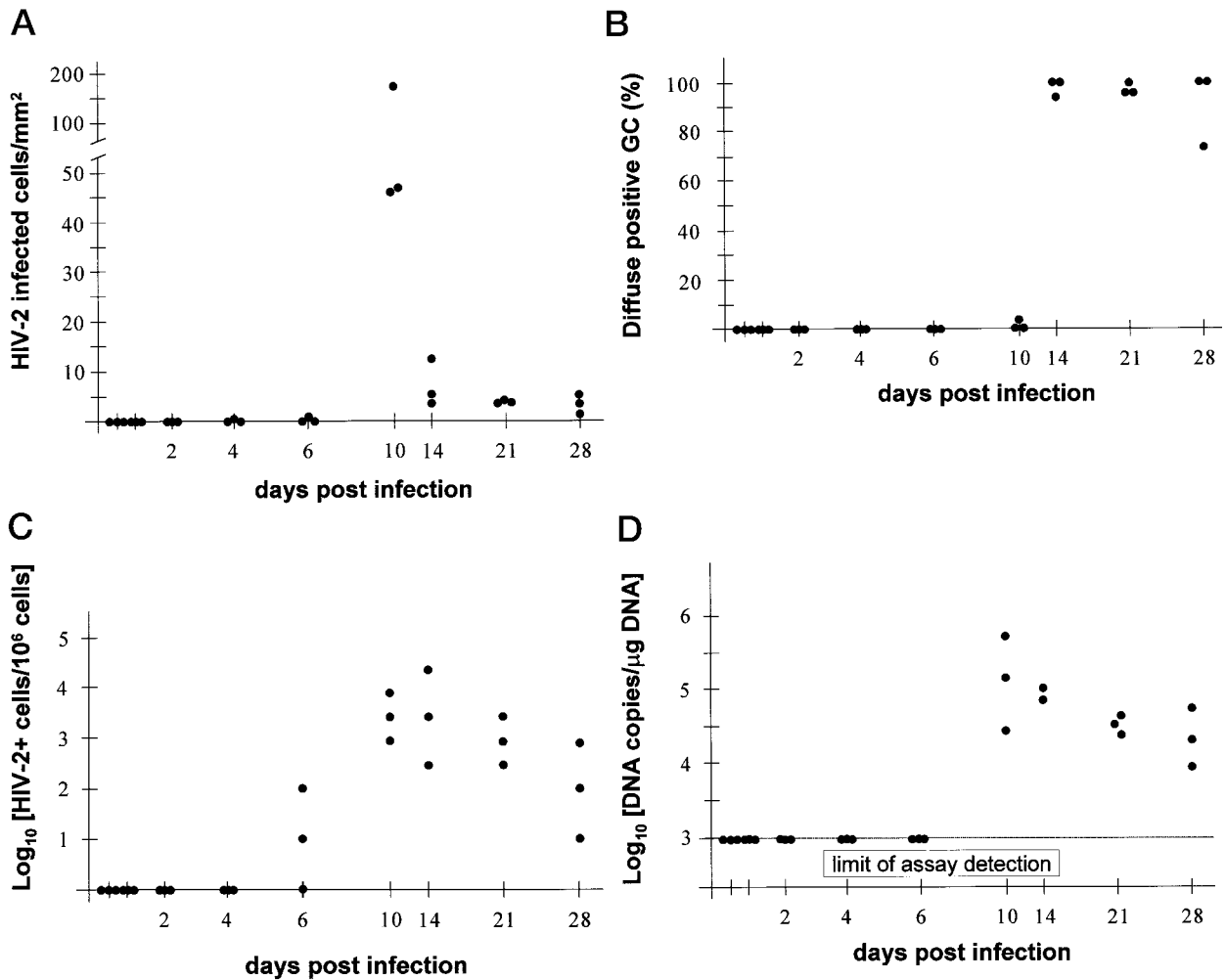


**Figure 2.** Detection of HIV-2-infected cells in mesenteric lymph nodes obtained from macaques between 12 hours and 28 days after experimental HIV-2 infection. **A:** HIV-2 RNA-expressing cells were identified in mesenteric lymph node sections by *in situ* hybridization for HIV-2 RNA after proteinase K treatment. **B:** HIV-2 RNA was detected in a diffuse distribution within germinal centers of mesenteric lymph nodes by *in situ* hybridization for HIV-2 RNA after combined heat plus proteinase K treatment. **C:** HIV-2-infected cells were identified in cells isolated from mesenteric lymph nodes by quantitative coculture. **D:** HIV-2 *gag* proviral DNA was detected in total DNA isolated from mesenteric lymph nodes by quantitative DNA PCR. For technical details see Materials and Methods section. Graphics illustrate individual data of each animal at necropsy.

bers of individual HIV-2-infected cells (46–175 positive cells/mm<sup>2</sup>; Figure 2A). These cells were distributed throughout all compartments of the lymph node, although a high density of HIV-2 RNA-expressing cells was seen within germinal centers (Figure 3, C–E) and the extrafollicular lymphoid tissue (Figure 3F). No preferential accumulation of HIV-2-infected cells within specific compartments of the lymph node was evident. We did not calculate the exact percentage of HIV-2 RNA-expressing cells, but we estimate that between 0.5 and 5% of the mesenteric lymph node cells were positive for HIV-2 RNA in the specimens obtained at 10 days after HIV-2 infection. Individual HIV-2 RNA-expressing cells were detectable in mesenteric lymph node sections of all animals euthanized at 14, 21, and 28 days after experimental infection (Figures 2A, 3G, and 3H). However, compared to the very high density of HIV-2 RNA+ cells at day 10, there was a very marked reduction in the number of individual HIV-2-infected cells at these later time points (Figure 2A). Again, the HIV-2 RNA-expressing cells at

days 14 and 28 were distributed throughout the entire lymph node without preference for a specific compartment of the lymph node (Figure 3, G and H).

Using *in situ* hybridization, after proteinase K plus heat treatment, HIV-2 RNA was undetectable in germinal centers of lymph nodes obtained from uninfected control animals and from macaques between 12 hours and 6 days after HIV-2 infection (Figure 2B). Apparent FDC-bound HIV-2 RNA, defined as diffuse *in situ* hybridization labeling over the germinal centers,<sup>3–5,7,36</sup> was first demonstrable in only a small percentage of germinal centers in just 1 of 3 animals at day 10 postinfection (Figure 2B). However, by day 14, HIV-2 RNA was identified in >90% of the germinal centers in mesenteric lymph nodes obtained from all three macaques (Figures 2B, 4A, and 4B). FDC-bound HIV-2 RNA persisted in germinal centers and was present in all animals examined 21 or 28 days after HIV-2 infection (Figures 2B and 4, C–F). Although the *in situ* hybridization procedure used for the detection of HIV-2 RNA does not allow an exact calculation of the

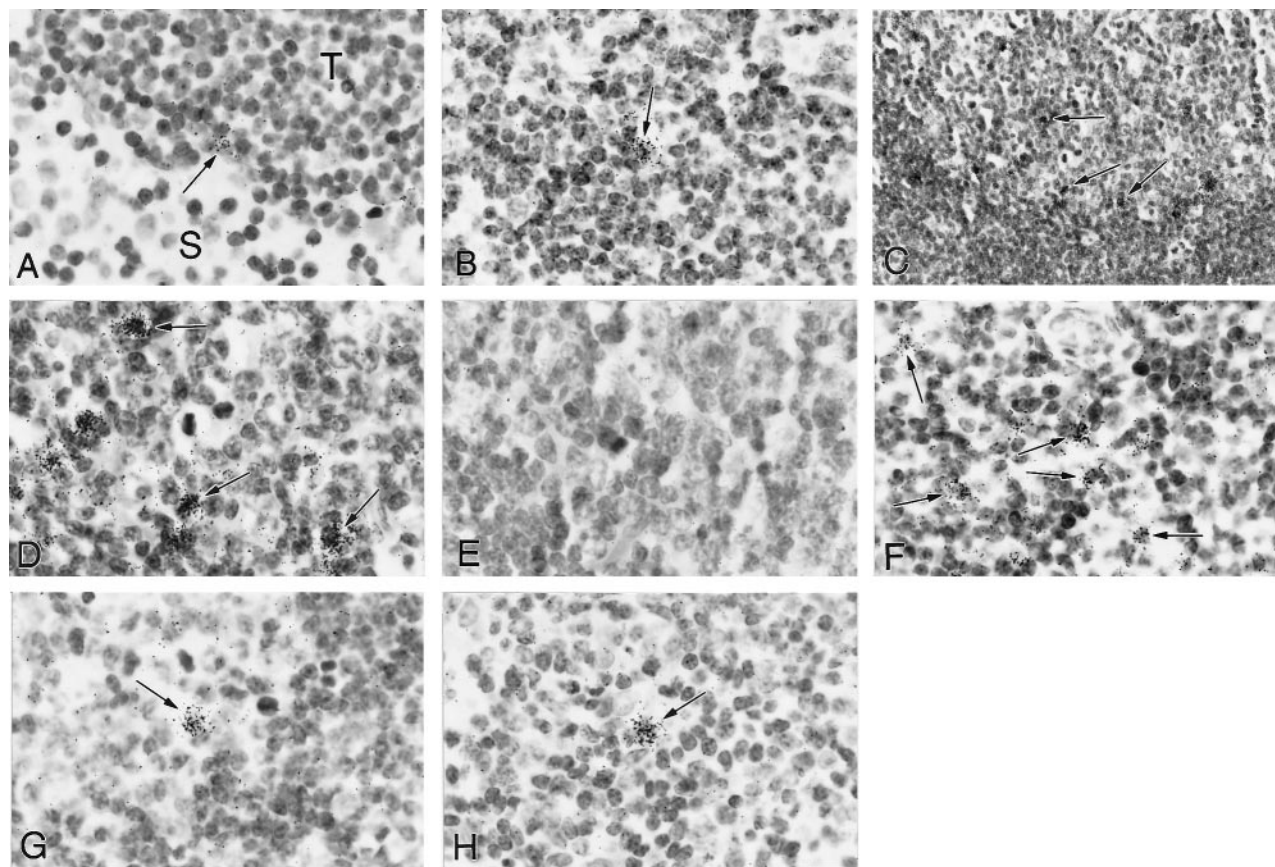


**Figure 3.** Detection of HIV-2-infected cells in macaque mesenteric lymph nodes by *in situ* hybridization. The *in situ* hybridization signal is visualized by black silver grains. **A:** A few HIV-2 RNA+ cells were detectable in 1 of 3 animals 4 days after HIV-2 infection. Individual HIV-2 RNA+ cell (arrow) at the border of the subcapsular sinus (S) and the adjacent interfollicular T lymphocyte-dependent zone (T). **B:** HIV-2 infected cell (arrow), located in the interfollicular T lymphocyte dependent zone, was seen in 1 of 3 animals 6 days after HIV-2 infection. **C and D:** Low and high power view of a germinal center obtained from a macaque 10 days after HIV-2 infection. Numerous individual HIV-2 RNA+ cells, some of which are indicated by arrows, can be identified throughout the germinal center. **E:** Hybridization signal is absent on the same mesenteric lymph node as illustrated in C and D with substitution of a sense probe in otherwise identical hybridization procedures used for C and D. **F:** Numerous individual HIV-2 RNA+ cells were identified throughout the interfollicular T lymphocyte-dependent zone in mesenteric lymph nodes obtained at 10 days after HIV-2 infection. Examples of HIV-2 RNA+ cells are indicated by arrows. **G:** Individual HIV-2 RNA+ cell (arrow) identified within a germinal center of a macaque mesenteric lymph node 21 days after HIV-2 infection and **(H)** within the T lymphocyte-dependent zone of a macaque mesenteric lymph node 28 days after HIV-2 infection. Hematoxylin and eosin counterstaining. Original magnifications,  $\times 1000$  (A, B, D–H) and  $\times 400$  (C).

amount of HIV-2 RNA, the germinal centers at 21 and 28 days postinfection had a marked increase of the *in situ* hybridization signal (number of silver grains) compared to those analyzed 10 and 14 days after infection. Thus, HIV-2 RNA is evident in a large number of individual cells outside the germinal centers at 10 days postinfection (Figure 2A), whereas widespread germinal center-associated HIV-2 is generally detected at day 14 (Figure 2B) in conjunction with the decline in individual HIV-2 RNA+ cells.

The presence of HIV-2-infected cells in mesenteric lymph nodes of the HIV-2-infected macaques was, furthermore, analyzed by quantitative coculture of mesenteric lymph node cells and by quantitative PCR of proviral HIV-2 DNA in total DNA isolated from lymph nodes obtained from all 27 macaques involved in this study.

The results of the quantitative coculture assays (Figure 2C), expressed as HIV-2-infected cells/ $10^6$  cells, closely correlated with the results of the *in situ* hybridization (Figure 2A), expressed as HIV-2-infected cells/ $\text{mm}^2$  of tissue. By the coculture technique, no HIV-2-infected cells were identified in mesenteric lymph node cells at 12 hours and

days 1, 2, and 4 after HIV-2 infection (Figure 2C). A small percentage of HIV-2-infected cells was evident at day 6 and again, the peak of HIV-2-infected cells occurred at day 10 (0.1–0.8% HIV-2-infected cells) to day 14 (0.03–2.4% HIV-2-infected cells), and decreased by days 21 and 28 (Figure 2C).

Quantitative PCR analyses for proviral HIV-2 DNA (Figure 2D), a marker for the number of HIV-2-infected cells rather than the amount of HIV-2 viral particles, confirmed the results of the *in situ* hybridization (Figure 2A) and the coculture (Figure 2C) experiments in identifying HIV-2-infected cells. DNA PCR analyses of specimens obtained between 12 hours and 6 days postinfection were below the limit of assay detection for HIV-2 DNA (Figure 2D). Again, the maximal concentration of proviral HIV-2 DNA was detectable at day 10 and declined somewhat thereafter (Figure 2D).

### Cellular Tropism of HIV-2

To identify which cells contained HIV-2 RNA, we combined immunohistochemical labeling of T lymphocytes,

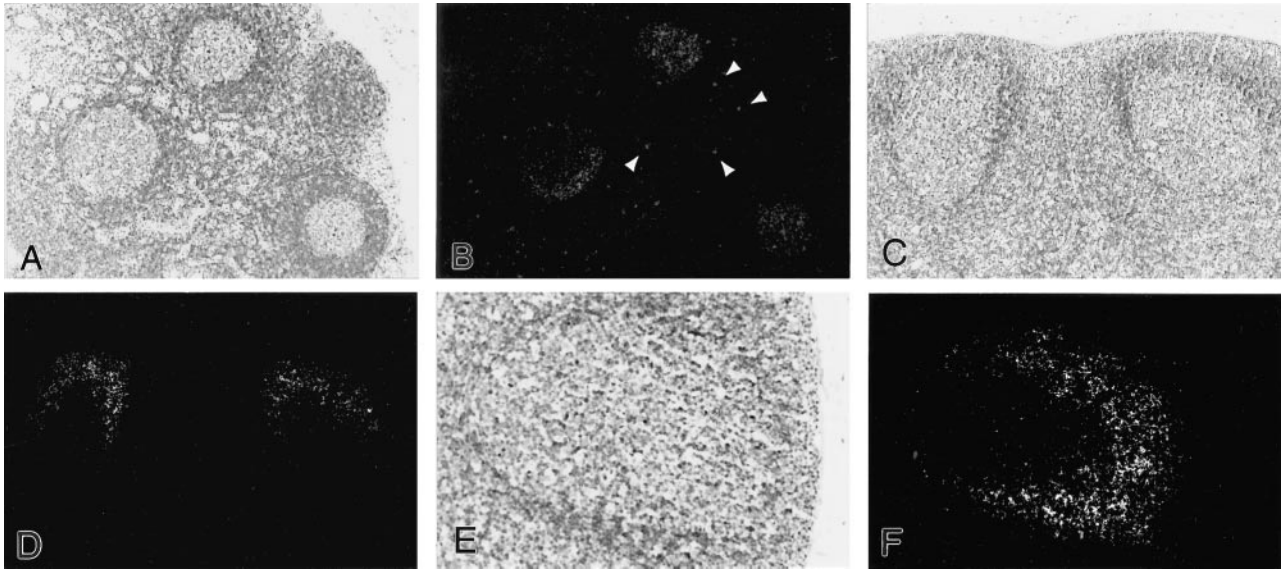


**Figure 4.** Detection of FDC-bound HIV-2 RNA in macaque mesenteric lymph nodes by *in situ* hybridization. Light field (A) and dark field (B) illustration of *in situ* hybridization for HIV-2 RNA in a mesenteric lymph node section 14 days after HIV-2 infection. Weak, diffuse labeling for HIV-2 RNA of all three illustrated germinal centers and additionally, detection of individual HIV-2 RNA+ cells within the extrafollicular T lymphocyte-dependent zone. Examples of individual HIV-2 RNA+ cells are indicated by arrowheads. Light field (C) and dark field (D) illustration of HIV-2 *in situ* hybridization in a macaque mesenteric lymph node obtained 21 days after HIV-2 infection. Strong diffuse labeling of HIV-2 RNA is detectable in almost all germinal centers in the analyzed specimens obtained from animals 21 and 28 days postinfection. Light field (E) and dark field (F) illustration of HIV-2 *in situ* hybridization in a macaque mesenteric lymph node 21 days postinfection. Strong diffuse labeling of HIV-2 RNA is primarily localized to the light zone of the germinal centers. Hematoxylin and eosin counterstaining. Original magnifications,  $\times 100$  (A–D) and  $\times 200$  (E and F).

macrophages, interdigitating dendritic cells, and FDCs, respectively, with *in situ* hybridization for HIV-2 RNA. Lymph nodes obtained between 12 hours and 2 days after HIV-2 infection were not included in this part of the study, because the previous experiments had failed to detect HIV-2-infected cells in mesenteric lymph nodes during that interval after HIV-2 infection.

Immunohistochemical labeling clearly identified the great majority of HIV-2 RNA+ cells as CD3+ T lymphocytes at all analyzed time points (Figure 5, A and B, and Table 1). However, a small percentage of HIV-2 RNA-expressing cells at all analyzed time points expressed phenotypic markers specific for macrophages (Figure 5C and Table 1) or interdigitating dendritic cells (Figure 5E and Table 1). Table 1 summarizes the results of the phenotypic characteristics of HIV-2-infected cells at the different time points analyzed. The proportional distribution of HIV-2-infected T lymphocytes, macrophages, and interdigitating dendritic cells did not show significant differences within the analyzed time frame.

Additionally, we combined immunohistochemical labeling of the FDC network with *in situ* hybridization for HIV-2 RNA (Figure 5, G and H). *In situ* hybridization was performed under conditions that were used for the detection of diffuse localization of HIV-2 RNA within germinal centers, eg, heat plus proteinase K treatment. Immunohistochemical labeling of macaque lymph nodes with the antibody to S-100 identified a network of positively staining cells within the germinal centers indistinguishable from the network of FDCs previously shown to be recognized by this antibody in human lymph node germinal centers.<sup>40</sup> Double labeling clearly demonstrated that the distribution of HIV-2 RNA within the germinal

centers mirrored the distribution of the FDC network of the germinal centers (Figure 5, G and H). However, the level of resolution of this double labeling procedure was not suitable to clearly discriminate between HIV-2 RNA localized within the cytoplasm or bound to the surface of FDC foot processes.

### Serology

Virus-specific IgA and IgG antibodies were initially detected in day 10 sera. These were not detectable at day 6 after infection. The virus-specific IgA levels peaked at day 10 and dropped to undetectable levels by day 28. Virus-specific IgG continued to rise after initial detection, peaking at day 21, and remained detectable at the conclusion of the study on day 28.

### Discussion

Lymphoid organs are considered to be major reservoirs harboring the HIV virus and are sites of HIV replication throughout the entire course of HIV-1 infection.<sup>1</sup> However, early events during the acute phase of HIV-1 infection have been difficult to study in HIV-infected humans, because most individuals are unaware of their HIV infection status soon after infection. The present study is the first to describe viral dissemination within lymphoid tissues during the acute infection phase in a model of human HIV infection involving nonhuman primates challenged with a pathogenic strain of HIV. Two clearly delineated chronological and anatomical stages of viral dissemination were defined within the first 28 days after

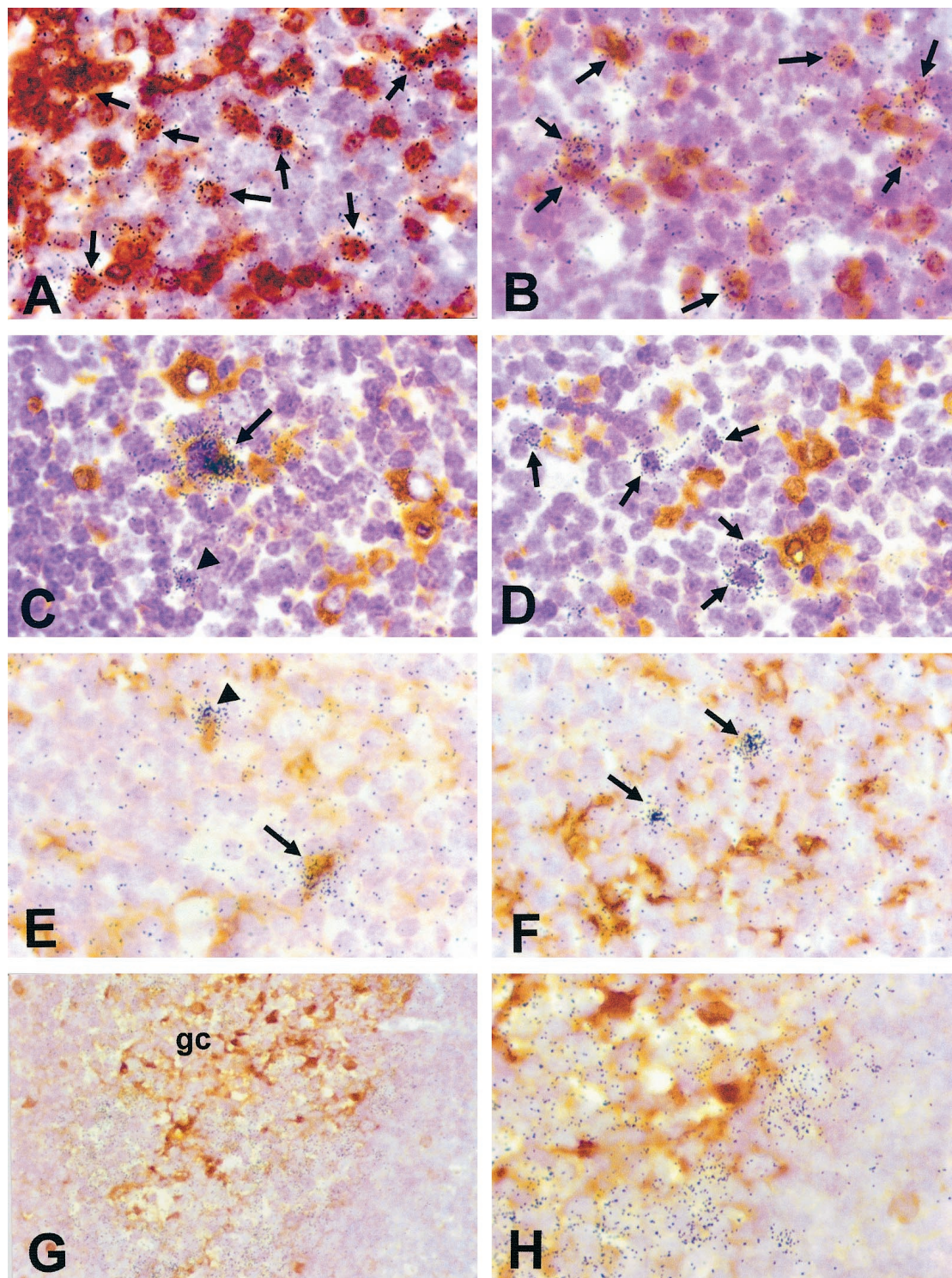


**Figure 5.** Phenotypes of HIV-2 infected cells. Combined *in situ* hybridization for HIV-2 RNA (black grains) with immunohistochemical labeling (brown) of CD3+ T lymphocytes (**A** and **B**), Ham56+ macrophages (**C** and **D**), p55+ interdigitating dendritic cells (**E** and **F**), and S100+ FDCs (**G** and **H**). **A** and **B**: Numerous individual HIV-2 RNA+ T lymphocytes were identified in mesenteric lymph node sections obtained from macaques 10 days postinfection. Examples of HIV-2 infected CD3+ T lymphocytes are indicated by **arrows**. **A**: Illustration of the border of a germinal center; T lymphocyte-dependent zone is located in the upper left corner and center of the germinal center is located in the lower right corner of the picture. **B**: Illustration of the center of a germinal center. **C**: HIV-2 RNA+ macrophage (**arrow**) and HIV-2 RNA+ cell negative for macrophage marker (**arrowhead**), within a germinal center of a macaque lymph node 10 days after HIV-2 infection. **D**: The majority of HIV-2 RNA+ cells (**arrows**) 10 days postinfection within the germinal centers, as illustrated here, and within the interfollicular tissue compartment (not shown), did not immunolabel as macrophages. **E**: HIV-2 RNA+ p55+ interdigitating dendritic cell (**arrow**) within the interfollicular T lymphocyte-dependent zone of a macaque lymph node 14 days after HIV-2 infection. A second illustrated HIV-2 RNA+ cell (**arrowhead**) did not immunolabel for p55, but was localized adjacent to a p55+ interdigitating dendritic cell. **F**: Same case as illustrated in **E** shows that the majority of HIV-2 RNA+ cells (**arrows**) did not express the p55 marker of interdigitating dendritic cells. **G**: Immunohistochemical labeling of S100 identifies the FDC network of a germinal center (gc) 21 days after HIV-2 infection. **H**: High power view of **G** demonstrates that HIV-2 RNA diffusely localized within the germinal center mirrors the distribution of the FDC network. Hematoxylin and eosin counterstaining. Original magnifications,  $\times 1000$  (**A–F, H**) and  $\times 400$  (**G**).

**Table 1.** Phenotypes of HIV-2 RNA-Expressing Cells

Time p.i. (days)	HIV-2 RNA+ T lymphocytes (%)	HIV-2 RNA+ macrophages (%)	HIV-2 RNA+ IDC (%)
6	80	0	0
10	96–98	0–4	0–1
14	94–100	0.5–3	0–1
21	90–100*	5–10	0–2
28	90–100*	1–8	0–2

Data obtained from combined immunohistochemistry and *in situ* hybridization as detailed in the Method section. Data are expressed as percent of the total number of HIV-2 RNA+ cells within the whole mesenteric lymph node section. Data represent the range obtained from the 3 different animals at each time point.

p.i., post-HIV-2 infection; IDC, interdigitating dendritic cells.

\*At days 21 and 28, the strong diffuse positive hybridization signal within the majority of the germinal centers did not allow clear identification of individual HIV-2 RNA+ cells within germinal centers in sections that were treated with heat plus proteinase K. The calculation of the percentage of HIV-2 RNA+ T lymphocytes at these time points was limited to T lymphocytes localized within the extrafollicular lymphoid tissue.

intravenous HIV-2<sub>287</sub> infection. First, a massive increase in individual HIV-2 infected cells, mostly T lymphocytes and a smaller percentage of macrophages and interdigitating dendritic cells, was identified within lymph nodes, a process that peaked at day 10 after HIV-2 infection. A shift in virus distribution was demonstrable between day 10 and day 14 after HIV-2 infection. At this later time point, HIV-2 RNA became predominantly localized to the FDC network of germinal centers as the number of individual HIV-2 RNA-expressing cells decreased. Thus, early in the natural history of infection, HIV-2 appears to go through a rapid, highly disseminated cellular phase and then localizes in the FDC network with relatively few infected cells present in other regions of the lymphoid tissue.

This discrete and narrow biological transition in the natural history of HIV infection, in which the site of infection in lymph nodes changes, offers a potential therapeutic window to interrupt progressive HIV infection. It has been speculated that maneuvers that interfere with the uptake of virus by the dendritic cell network may prevent the establishment of a stable reservoir of infection.<sup>1,11</sup> A major finding of our studies is evidence that such maneuvers may need to be used very early in HIV infection to be successful, and that the therapeutic window to prevent uptake of virus by dendritic cells is chronologically very narrow.

Our current knowledge of HIV-1 dissemination in peripheral lymphoid tissue during acute or asymptomatic early infection in humans is very limited. Pantaleo et al reported a time-dependent transition of HIV-1 within the lymph node microenvironment of HIV-1-infected individuals.<sup>41</sup> In subjects with primary infections, HIV was present mostly in individual virus-expressing cells, and trapping of virions in the FDC network was minimal or absent.<sup>41</sup> However, FDC-bound HIV was the predominant form of HIV detected in lymph nodes obtained from patients after 4 months of primary infection, and the numbers of individual virus-expressing cells were significantly lower in subjects with long-term infection.<sup>41</sup> Phenotypes

of HIV-1-infected cells were not evaluated in that study. In another study, Tenner-Racz and coworkers identified both productively infected individual cells and extensive HIV-1 RNA retention on the FDC network of germinal centers in lymph nodes from asymptomatic HIV-1-infected patients.<sup>36</sup> Differences in HIV-1 distribution patterns occurring over time were not reported.<sup>36</sup> Some of the differences between these two studies may be the result of examining lymph nodes from patients at different stages of their infection and hence at different points in their immune response to the virus. In the study by Tenner-Racz et al,<sup>36</sup> HIV-1 RNA-expressing cells were identified as CD4+ T cells in germinal centers and in the extrafollicular lymphatic tissue, whereas HIV-1 RNA was undetectable in natural killer cells, monocytes/macrophages, or dendritic cells. Other studies that have investigated viral distribution patterns in lymph nodes obtained from HIV-1-infected individuals have generally been limited to specimens obtained at later stages of HIV-1 infection.<sup>2–4,6,7,42,43</sup> These studies of later stages of infection showed that HIV-1 RNA and protein localize predominantly to the FDC network of germinal centers. Variable numbers of individual HIV-1-infected cells have been found in the lymph nodes, that were identified as either T lymphocytes<sup>4,6,43</sup> or macrophages.<sup>3,6,43</sup>

This study in nonhuman primate species susceptible to HIV-2 infection allows the most precise description to date of the sequence of infection in lymphoid tissues involving a lentivirus pathogenic to humans. *M. nemestrina* inoculated with HIV-2<sub>287</sub> develop high virus loads, rapid CD4+ cell depletion to <200/ $\mu$ l within a few weeks postinoculation, and a predictable, rapid progression to AIDS within months after inoculation.<sup>18,20,22</sup> Necropsy findings in HIV-2<sub>287</sub>-infected macaques include cases of encephalomeningitis, interstitial pneumonia, and microvascular thrombotic microangiopathy,<sup>39</sup> substantiating the validity of this model of HIV infection. Our data showing two time-dependent patterns of viral dissemination within lymph nodes were highly consistent among the different animals at each of the analyzed time points, and the use of independent techniques for the detection of HIV-2-infected cells (coculture, PCR, *in situ* hybridization) showed an excellent correlation in each of the animals. Early in the course of infection, HIV-2<sub>287</sub> predominantly infected T lymphocytes, but macrophages and bone marrow-derived dendritic cells were identified as additional cellular targets of HIV-2<sub>287</sub> *in vivo*. Whether a shift in the cellular tropism of HIV-2 might occur during chronic stages of HIV-2 infection will be determined in subsequent studies that are currently being performed.

Viral dissemination in lymphoid tissues has also been investigated in SIV-infected nonhuman primates. Chakrabarti et al identified two phases of viral spread in lymph nodes from rhesus macaques after intravenous and intracranial SIV<sub>mac251</sub> infection.<sup>44</sup> Although high numbers of individual SIV-infected cells, mostly monocytes/macrophages, were identified in lymph nodes at 7 and 14 days after infection, SIV RNA predominantly localized to the FDC network of germinal centers by 2 weeks after inoculation.<sup>44</sup> Other groups detected peak numbers of individual SIV-infected cells

in lymph nodes from rhesus macaques at about 2 weeks post-SIV<sub>mac251</sub><sup>45</sup> or SIV<sub>mac239</sub><sup>46</sup> infection that subsequently declined. Detection of germinal center-associated SIV was not reported in those studies. Results obtained from SIV-based models may not be directly applicable to infection with human lentiviruses. The predominant infection of monocytes/macrophages in lymph nodes in SIV<sub>mac251</sub>-challenged macaques that has been reported previously<sup>44</sup> is contrary to findings in lymphoid tissues of HIV-1-infected humans where T lymphocytes represent the major cellular targets.<sup>4,6,36</sup> However, a recent report indicates that SIV<sub>mac251</sub> preferentially localizes in CD4+ T cells in lymph nodes during the first 7 days of experimental infection of macaques.<sup>47</sup>

In conclusion, our data further strengthen the potential importance of the HIV-2<sub>287</sub> *M. nemestrina* model for human HIV infection in general. The model involves a human pathogen and reproducibly induces an immunodeficiency syndrome in an accelerated time frame. The in-depth evaluation of immunopathogenic events in the early phase after HIV-2 challenge revealed that viral dissemination in lymphoid tissue follows a consistent time-dependent pattern in this model system. Furthermore, the time-dependent patterns of viral distribution and the cellular targets of HIV-2<sub>287</sub> infection are in agreement with reported findings in HIV-1-infected humans. Our findings demonstrate an early movement of virus from infected cells into lymphoid germinal centers, a process thought to be a major component of viral latency and viral persistence in the face of antiretroviral therapy. Because the findings in the lymph nodes of HIV-2-infected macaques are generally similar to what has been inferred from humans, albeit occurring in an accelerated fashion, this pattern of shifting virus localization may represent a major obstacle to virus eradication and development of a cure for HIV infection in individuals who do not receive effective treatment early in the disease process. Alternately, the early movement of virus into the FDC network may be a protective event that ameliorates early dissemination of the virus and/or is a consequence of virus trapping by FDC of virus complexed to anti-HIV antibodies. The available data, including the data from this study, do not clearly establish which of these possibilities is most likely to be correct. The HIV-2<sub>287</sub> *M. nemestrina* model offers outstanding opportunities for testing of intervention and vaccine strategies designed to interrupt this sequence of lymphoid infection, and to investigate whether this sequence protects or harms the health of the HIV-infected host.

### Acknowledgments

We thank Drs. Michael E. Rosenfeld of the Department of Pathobiology and Paul A.J. Brown of the Department of Pathology (University of Washington, Seattle) for technical assistance with the computer-assisted morphometry analysis. Provision of reagents by the AIDS Research and Reagents Program of the National Institute of Allergy and Infectious Diseases, National Institutes of Health, is gratefully acknowledged.

### References

1. Pantaleo G, Graziosi C, Demarest JF, Cohen OJ, Vaccarezza M, Gantt K, Muro-Cacho C, Fauci AS: Role of lymphoid organs in the pathogenesis of human immunodeficiency virus (HIV) infection. *Immunol Rev* 1994, 140:105-130
2. Emilie D, Peuchmaur M, Maillot MC, Crevon MC, Brousse N, Del-fraissy JF, Dromont J, Galanaud P: Production of interleukins in human immunodeficiency virus-1-replicating lymph nodes. *J Clin Invest* 1990, 86:148-159
3. Fox CH, Tenner-Racz K, Racz P, Firpo A, Pizzo PA, Fauci AS: Lymphoid germinal centers are reservoirs of human immunodeficiency virus type 1 RNA. *J Infect Dis* 1991, 164:1051-1057
4. Spiegel H, Herbst H, Niedobitek G, Foss HD, Stein H: Follicular dendritic cells are a major reservoir for human immunodeficiency virus type 1 in lymphoid tissues facilitating infection of CD4+ T-helper cells. *Am J Pathol* 1992, 140:15-22
5. Pantaleo G, Graziosi C, Demarest JF, Butini L, Montroni M, Fox CH, Orenstein JM, Kotler DP, Fauci AS: HIV infection is active and progressive in lymphoid tissue during the clinically latent stage of disease. *Nature* 1993, 362:355-358
6. Embretson J, Zupancic M, Ribas JL, Burke A, Racz P, Tenner-Racz K, Haase AT: Massive covert infection of helper T lymphocytes and macrophages by HIV during the incubation period of AIDS. *Nature* 1993, 362:359-362
7. Burke AP, Benson W, Ribas JL, Anderson D, Chu WS, Smialek J, Virmani R: Postmortem localization of HIV-1 RNA by in situ hybridization in lymphoid tissues of intravenous drug addicts who died unexpectedly. *Am J Pathol* 1993, 142:1701-1713
8. Haase AT, Henry K, Zupancic M, Sedgewick G, Faust RA, Melroe H, Cavert W, Gebhard K, Staskus K, Zhang ZQ, Dailey PJ, Balfour HH, Jr., Erice A, Perelson AS: Quantitative image analysis of HIV-1 infection in lymphoid tissue. *Science* 1996, 274:985-989
9. Tenner-Racz K, von Stemm AM, Guhlk B, Schmitz J, Racz P: Are follicular dendritic cells, macrophages and interdigitating cells of the lymphoid tissue productively infected by HIV? *Res Virol* 1994, 145:177-182
10. Bell D, Young JW, Banchereau J: Dendritic cells. *Adv Immunol* 1999, 72:255-324
11. Tenner-Racz K, Racz P: Follicular dendritic cells initiate and maintain infection of the germinal centers by human immunodeficiency virus. *Curr Top Microbiol Immunol* 1995, 201:141-159
12. Cameron P, Pope M, Granelli-Piperno A, Steinman RM: Dendritic cells and the replication of HIV-1. *J Leukoc Biol* 1996, 59:158-171
13. Grouard G, Clark EA: Role of dendritic and follicular dendritic cells in HIV infection and pathogenesis. *Curr Opin Immunol* 1997, 9:563-567
14. Heath SL, Tew JG, Szakal AK, Burton GF: Follicular dendritic cells and human immunodeficiency virus infectivity. *Nature* 1995, 377:740-744
15. Graziosi C, Soudeyns H, Rizzardi GP, Bart PA, Chapuis A, Pantaleo G: Immunopathogenesis of HIV infection. *AIDS Res Hum Retroviruses* 1998, 14(suppl 2):S135-S142
16. Letvin NL: Animal models for AIDS. *Immunol Today* 1990, 11:322-326
17. Fultz PN: Nonhuman primate models for AIDS. *Clin Infect Dis* 1993, 17 Suppl 1:S230-S235
18. Levy JA: The value of primate models for studying human immunodeficiency virus pathogenesis. *J Med Primatol* 1996, 25:163-174
19. McClure J, Scheibel M, Steele J, Dorofeeva N, Schmidt A, Hu SL, Morton W: HIV-2 macaque model for HIV infection and pathogenesis: *J Med Primatol* 1994, 23:244-245
20. Looney DJ, McClure J, Kent SJ, Radaelli A, Kraus G, Schmidt A, Steffy K, Greenberg P, Hu SL, Morton WR, Wong-Staal F: A minimally replicative HIV-2 live-virus vaccine protects *M. nemestrina* from disease after HIV-2(287) challenge. *Virology* 1998, 242:150-160
21. Rey-Cuille MA, Galabru J, Laurent-Crawford A, Krust B, Montagnier L, Hovanessian AG: HIV-2 EHO isolate has a divergent envelope gene and induces single cell killing by apoptosis. *Virology* 1994, 202, 471-476
22. Watson A, McClure J, Ranchalis J, Scheibel M, Schmidt A, Kennedy B, Morton WR, Haigwood NL, Hu SL: Early postinfection antiviral treatment reduces viral load and prevents CD4+ cell decline in HIV type 2-infected macaques. *AIDS Res Hum Retroviruses* 1997, 13:1375-1381
23. Hollinger FB, Bremer JW, Myers LE, Gold JW, McQuay L: Standard-

- ization of sensitive human immunodeficiency virus coculture procedures and establishment of a multicenter quality assurance program for the AIDS Clinical Trials Group. *J Clin Microbiol* 1992, 30:1787-1794
24. Vanden Heuvel JP, Tyson FL, Bell DA: Construction of recombinant RNA templates for use as internal standards in quantitative RT-PCR. *Biotechniques* 1993, 14:395-398
  25. Mason DY, Cordell J, Brown M, Pallesen G, Ralfkiaer E, Rothbard J, Crumpton M, Gatter KC: Detection of T cells in paraffin wax embedded tissue using antibodies against a peptide sequence from the CD3 antigen. *J Clin Pathol* 1989, 42:1194-1200
  26. Gown AM, Tsukada T, Ross R: Human atherosclerosis. II. Immunocytochemical analysis of the cellular composition of human atherosclerotic lesions. *Am J Pathol* 1986, 125:191-207
  27. Cocchia D, Tiberio G, Santarelli R, Michetti F: S-100 protein in "follicular dendritic" cells of rat lymphoid organs. An immunochemical and immunocytochemical study. *Cell Tissue Res* 1983, 230:95-103
  28. Vanstapel MJ, Gatter KC, de Wolf-Peeters C, Mason DY, Desmet VD: New sites of human S-100 immunoreactivity detected with monoclonal antibodies. *Am J Clin Pathol* 1986, 85:160-168
  29. Mosialos G, Birkenbach M, Ayejunie S, Matsumura F, Pinkus GS, Kieff E, Langhoff E: Circulating human dendritic cells differentially express high levels of a 55-kd actin-bundling protein. *Am J Pathol* 1996, 148:593-600
  30. Yamashiro-Matsumura S, Matsumura F: Purification and characterization of an F-actin-bundling 55-kilodalton protein from HeLa cells. *J Biol Chem* 1985, 260:5087-5097
  31. Hu J, Pope M, Brown C, O'Doherty U, Miller CJ: Immunophenotypic characterization of simian immunodeficiency virus-infected dendritic cells in cervix, vagina, and draining lymph nodes of rhesus monkeys. *Lab Invest* 1998, 78:435-451
  32. Eitner F, Cui Y, Hudkins KL, Anderson DM, Schmidt A, Morton WR, Alpers CE: Chemokine receptor (CCR5) expression in human kidneys and in the HIV infected macaque. *Kidney Int* 1998, 54:1945-1954
  33. Alpers CE, Hudkins KL, Davis CL, Marsh CL, Riches W, McCarty JM, Genjamin CD, Carlos TM, Harlan JM, Lobb R: Expression of vascular cell adhesion molecule-1 in kidney allograft rejection. *Kidney Int* 1993, 44:805-816
  34. Alpers CE, Davis CL, Barr D, Marsh CL, Hudkins KL: Identification of platelet-derived growth factor A and B chains in human renal vascular rejection. *Am J Pathol* 1996, 148:439-451
  35. Crawford RS, Kirk EA, Rosenfeld ME, LeBoeuf RC, Chait A: Dietary antioxidants inhibit development of fatty streak lesions in the LDL receptor-deficient mouse. *Arterioscler Thromb Vasc Biol* 1998, 18:1506-1513
  36. Tenner-Racz K, Stellbrink HJ, van Lunzen J, Schneider C, Jacobs JP, Raschdorff B, Grosschupff G, Steinman RM, Racz P: The unenlarged lymph nodes of HIV-1-infected, asymptomatic patients with high CD4 T cell counts are sites for virus replication and CD4 T cell proliferation. The impact of highly active antiretroviral therapy. *J Exp Med* 1998, 187:949-959
  37. Eitner F, Cui Y, Hudkins KL, Alpers CE: Chemokine receptor (CXCR4) mRNA expressing leukocytes are increased in human renal allograft rejection. *Transplantation* 1998, 66:1551-1557
  38. Kuller L, Thompson J, Watanabe R, Iskandriati D, Alpers CE, Morton WR, Agy MB: Mucosal antibody expression following rapid SIV(Mne) dissemination in intrarectally infected Macaca nemestrina. *AIDS Res Hum Retroviruses* 1998, 14:1345-1356
  39. Eitner F, Cui Y, Hudkins KL, Schmidt A, Birkebak T, Agy MB, Hu SL, Morton WR, Anderson DM, Alpers CE: Thrombotic microangiopathy in the HIV-2 infected macaque. *Am J Pathol* 1999, 155:649-661
  40. Carbone A, Poletti A, Manconi R, Volpe R, Santi L: Demonstration of S-100 protein distribution in human lymphoid tissues by the avidin-biotin complex immunostaining method. *Hum Pathol* 1985, 16:1157-1164
  41. Pantaleo G, Cohen OJ, Schacker T, Vaccarezza M, Graziosi C, Rizzardi GP, Kahn J, Fox CH, Schnittman SM, Schwartz DH, Corey L, Fauci AS: Evolutionary pattern of human immunodeficiency virus (HIV) replication and distribution in lymph nodes following primary infection: implications for antiviral therapy. *Nat Med* 1998, 4:341-345
  42. Tenner-Racz K, Racz P, Bofill M, Schulz-Meyer A, Dietrich M, Kern P, Weber J, Pinching AJ, Veronese-Dimarzo F, Popovic M, Klatzmann D, Gluckman JC, Janossy G: HTLV-III/LAV viral antigens in lymph nodes of homosexual men with persistent generalized lymphadenopathy and AIDS. *Am J Pathol* 1986, 123:9-15
  43. Soontornniyomkij V, Wang G, Kapadia SB, Achim CL, Wiley CA: Confocal microscopy assessment of lymphoid tissues with follicular hyperplasia from patients infected with human immunodeficiency virus type 1. *Arch Pathol Lab Med* 1998, 122:534-538
  44. Chakrabarti L, Isola P, Cumont MC, Claessens-Maire MA, Hurtrel M, Montagnier L, Hurtrel B: Early stages of simian immunodeficiency virus infection in lymph nodes. Evidence for high viral load and successive populations of target cells. *Am J Pathol* 1994, 144:1226-1237
  45. Reimann KA, Tenner-Racz K, Racz P, Montefiori DC, Yasutomi Y, Lin W, Ransil BJ, Letvin NL: Immunopathogenic events in acute infection of rhesus monkeys with simian immunodeficiency virus of macaques. *J Virol* 1994, 68:2362-2370
  46. Lackner AA, Vogel P, Ramos RA, Kluge JD, Marthas M: Early events in tissues during infection with pathogenic (SIVmac239) and non-pathogenic (SIVmac1A11) molecular clones of simian immunodeficiency virus. *Am J Pathol* 1994, 145:428-439
  47. Stahl-Hennig C, Steinman RM, Tenner-Racz K, Pope M, Stolte N, Matz-Rensing K, Grobschupff G, Raschdorff B, Hunsmann G, Racz P: Rapid infection of oral mucosal-associated lymphoid tissue with simian immunodeficiency virus. *Science* 1999, 285:1261-1265